# Recent highlights of CPV measurements in B decays at LHCb

钱文斌（Wenbin Qian）
中国科学院大学（University of Chinese Academy of Sciences）
2019/07/30
呼和浩特

**第17届全国重味物理和CP破坏研讨会**

# Matter-antimatter asymmetry

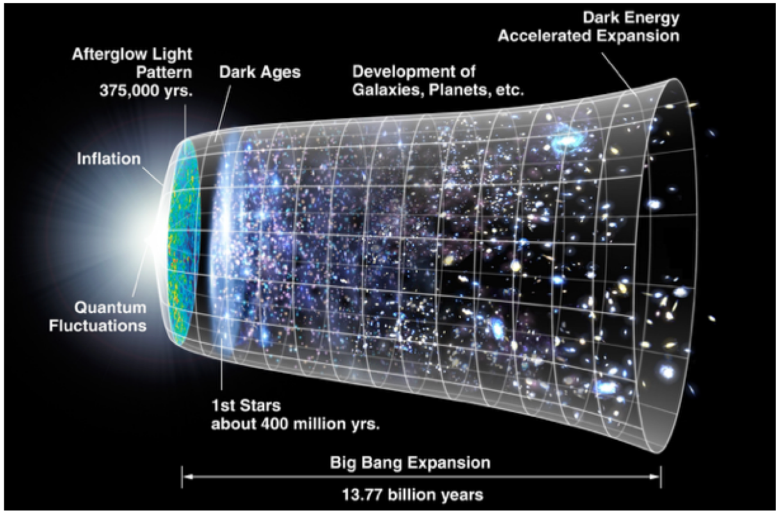



- Central question of flavor physics: how the Universe develops into current matter-dominated state from Big Bang

- Sakharov conditions: C and CP violation required

- Current SM: CKM mechanism, but orders of magnitude smaller! Need to search for new sources of CPV

# Global fit



- CPV in SM described by CKM mechanism
- Precision measurements ⇨ global fit

**SM baseline，$\gamma$ least precise measurement**

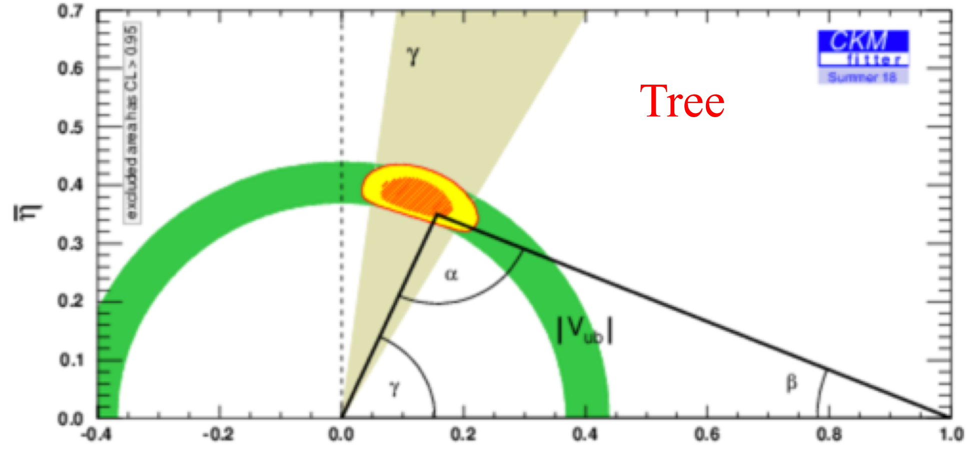


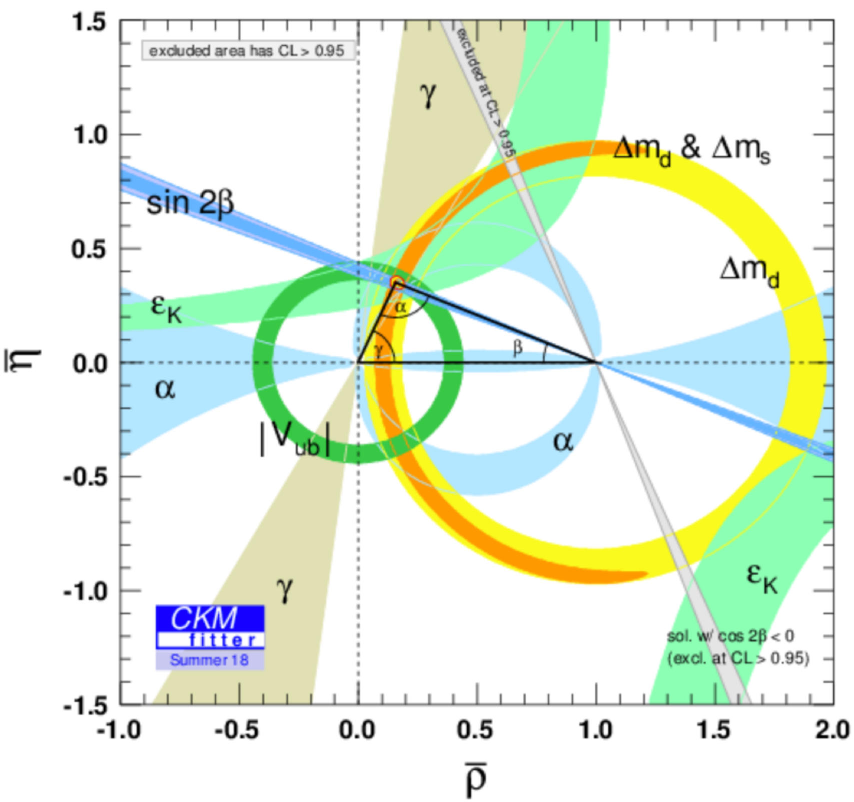


**$\phi_s$, a probe of new physics**

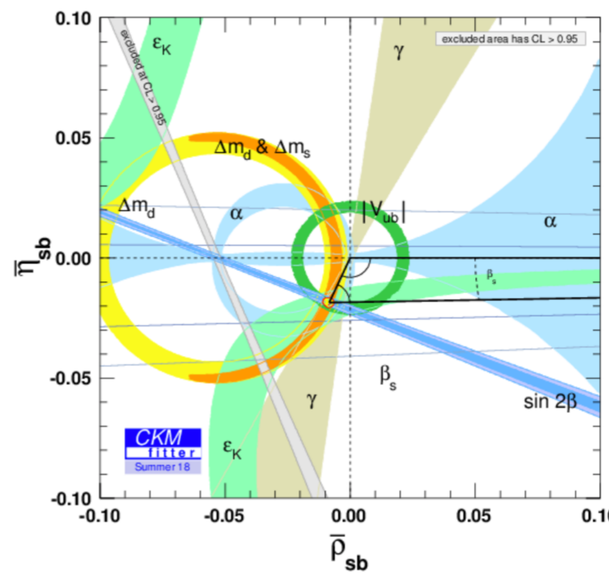

# Angle $\gamma$

- CPV in SM $\propto \sin\gamma$, key element of CKM matrix (mechanism) **PRL 55 (1985) 1039**
- Least well known CKM parameters before LHCb, bottle net for understanding CKM mechanism

$$\gamma = \arg\left[-V_{ud}V_{ub}^{*}/(V_{cd}V_{cb}^{*})\right]$$

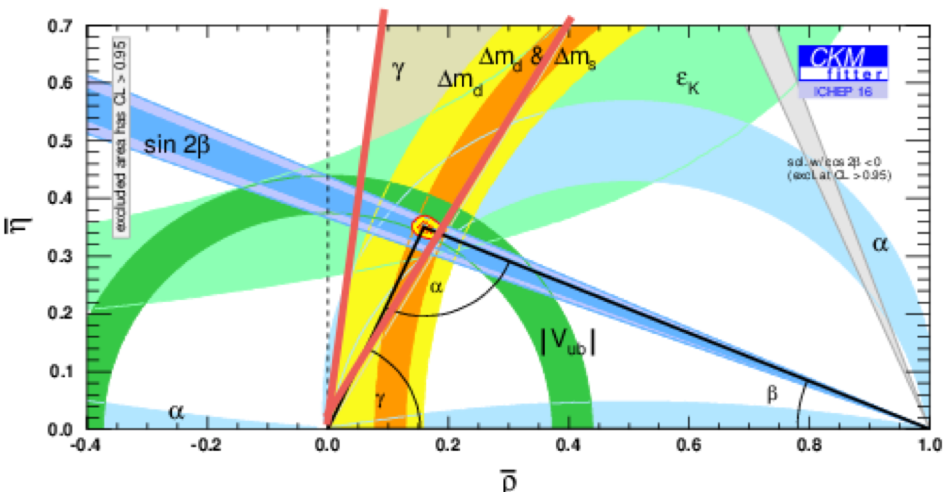


**Direct:** $\gamma = (73.5^{+4.3}_{-5.0})^{\circ}$

**VS**

**Indirect:** $\gamma = (65.3^{+1.0}_{-2.5})^{\circ}$

**New Physics?**

- $\gamma$ at tree level: clean theory prediction, $\delta\gamma/\gamma \sim 10^{-7}$ **JHEP 1401 (2014) 051**

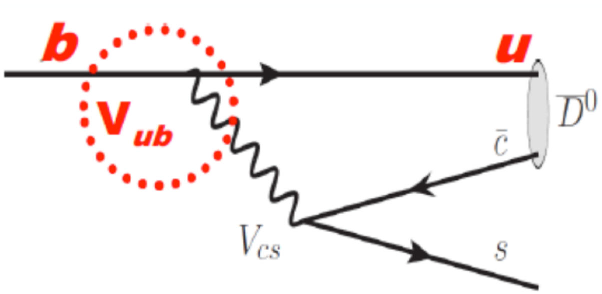


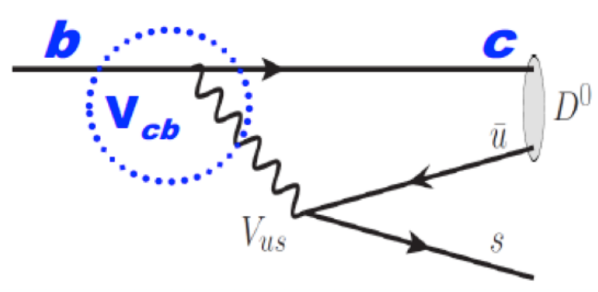

# Continuing efforts from LHCb

- LHCb reduces its uncertainties by more than a factor of 2 and will do more

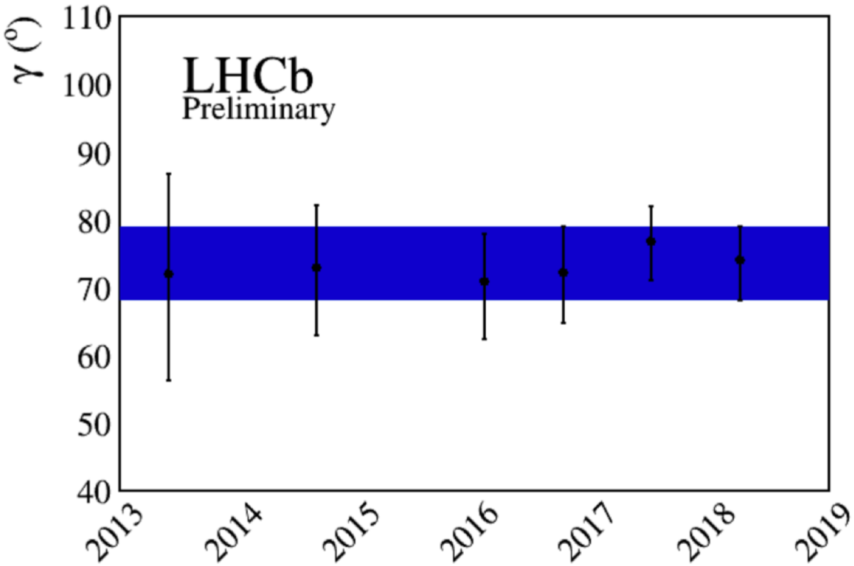


- Tree-level $\gamma$： sensitive channels ($B \to D^{(*)}h(h)$ etc.) with small BFs, need to combined them to achieve best sensitivity

| $B$ decay | $D$ decay | Method | Ref. | Dataset[†] |
|---|---|---|---|---|
| $B^+ \to DK^+$ | $D \to h^+h^-$ | GLW | [14] | Run 1 & 2 |
| $B^+ \to DK^+$ | $D \to h^+h^-$ | ADS | [15] | Run 1 |
| $B^+ \to DK^+$ | $D \to h^+\pi^-\pi^+\pi^-$ | GLW/ADS | [15] | Run 1 |
| $B^+ \to DK^+$ | $D \to h^+h^-\pi^0$ | GLW/ADS | [16] | Run 1 |
| $B^+ \to DK^+$ | $D \to K^0_S h^+h^-$ | GGSZ | [17] | Run 1 |
| $B^+ \to DK^+$ | $D \to K^0_S h^+h^-$ | GGSZ | [18] | Run 2 |
| $B^+ \to DK^+$ | $D \to K^0_S K^+\pi^-$ | GLS | [19] | Run 1 |
| $B^+ \to D^*K^+$ | $D \to h^+h^-$ | GLW | [14] | Run 1 & 2 |
| $B^+ \to DK^{*+}$ | $D \to h^+h^-$ | GLW/ADS | [20] | Run 1 & 2 |
| $B^+ \to DK^{*+}$ | $D \to h^+\pi^-\pi^+\pi^-$ | GLW/ADS | [20] | Run 1 & 2 |
| $B^+ \to DK^+\pi^+\pi^-$ | $D \to h^+h^-$ | GLW/ADS | [21] | Run 1 |
| $B^0 \to DK^{*0}$ | $D \to K^+\pi^-$ | ADS | [22] | Run 1 |
| $B^0 \to DK^+\pi^-$ | $D \to h^+h^-$ | GLW-Dalitz | [23] | Run 1 |
| $B^0 \to DK^{*0}$ | $D \to K^0_S\pi^+\pi^-$ | GGSZ | [24] | Run 1 |
| $B^0_s \to D_s^{\mp}K^{\pm}$ | $D_s^+ \to h^+h^-\pi^+$ | TD | [25] | Run 1 |
| $B^0 \to D^{\mp}\pi^{\pm}$ | $D^+ \to K^+\pi^-\pi^+$ | TD | [26] | Run 1 |

# Updates from $B^0 \to DK^*, D \to hh, 4h$

LHCb-PAPER-2019-021

4.8 $fb^{-1}$

- Updates from previous 3 $fb^{-1}$ analysis with $D \to 2h$, and Dalitz plot analysis of $B \to DK\pi$

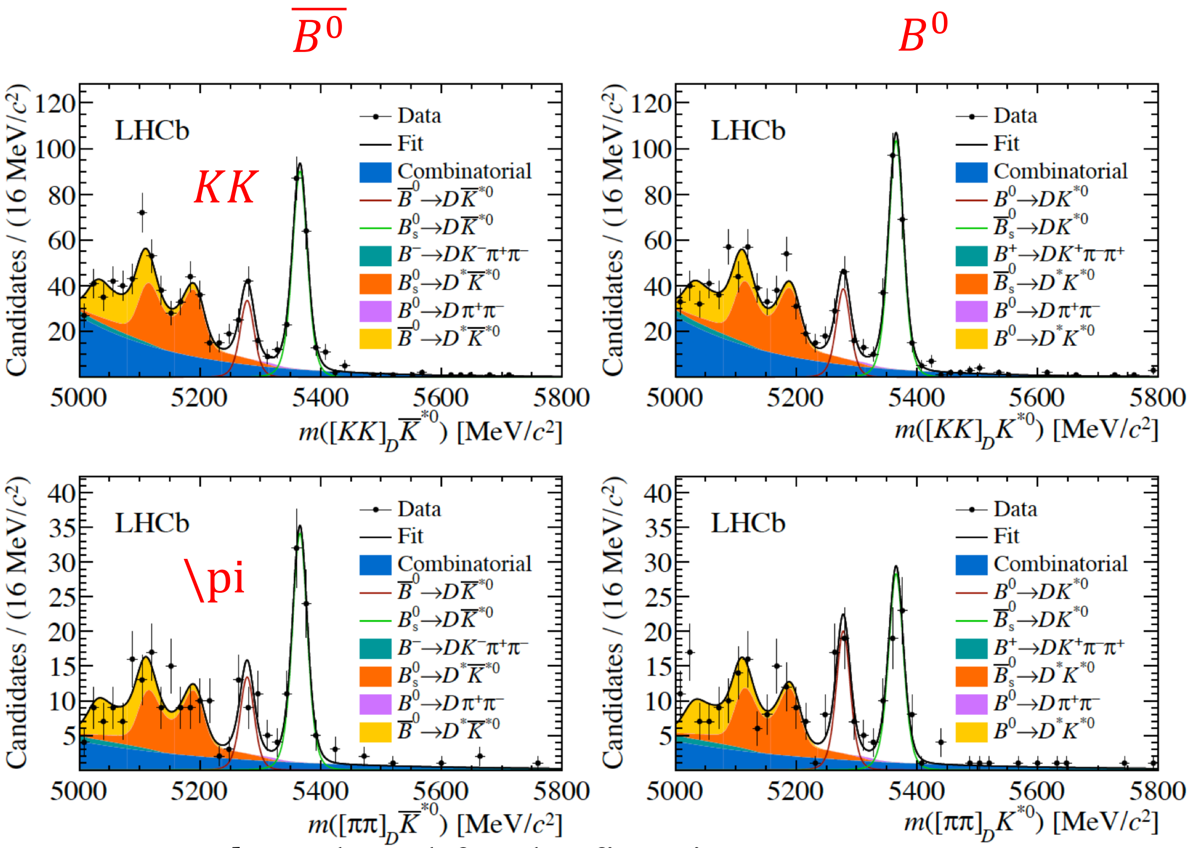


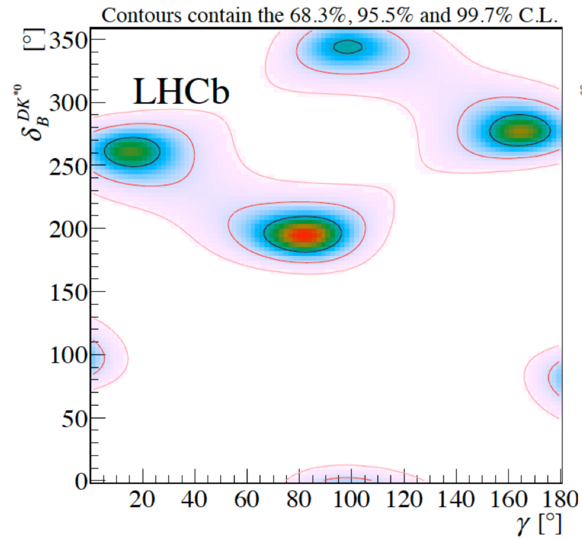


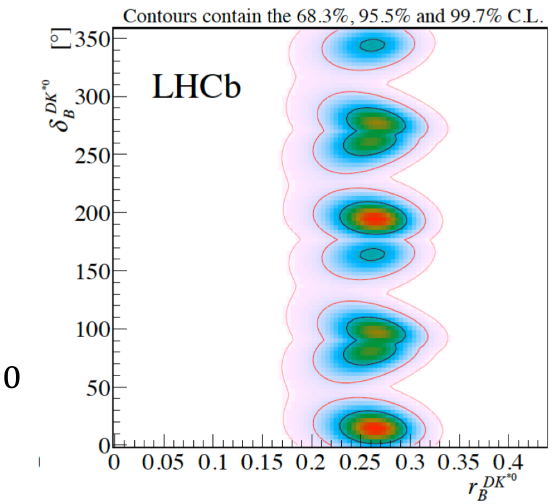


- $D \to 4h$ analyzed for the first time
- First discovery on $B^0 \to D(\pi^+K^-)K^{*0}$ and $B^0 \to D(4\pi)K^{*0}$
- $r_B^{DK^{*0}}$ constrained to $0.265 \pm 0.023$

# Other activities

Phys. Rev. D 98 (2018) 072006
Phys. Rev. D 98 (2018) 071103(R)

- $B^0 \to \overline{D^0}KK$ and $B_s \to \overline{D^0}KK$ decays
  - Time-Dependent Dalitz analyses to access CKM angle $\gamma$ and $\beta_{(s)}$
  - Not only probe $\sin 2\beta_{(s)}$, but also $\cos 2\beta_{(s)}$
  - Dalitz structures interesting for charm spectroscopy studies
- $B_s \to D^{(*)}\phi$ decays: special cases where final states are in CP eigenstates

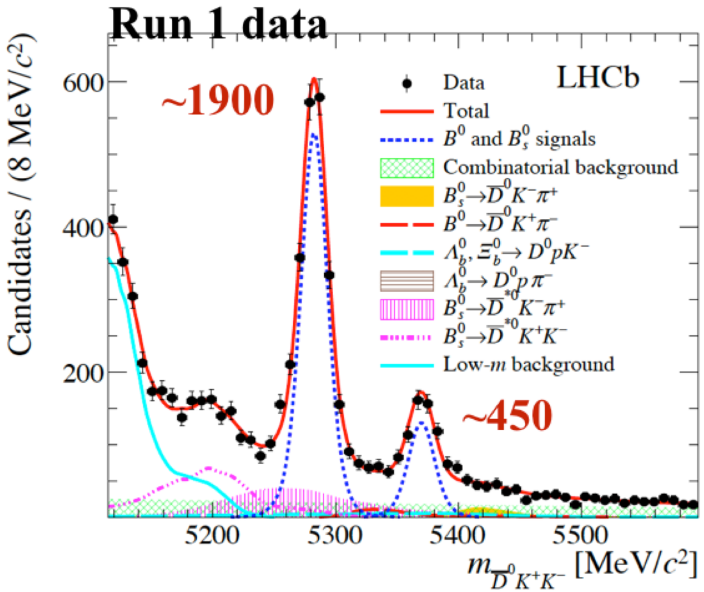


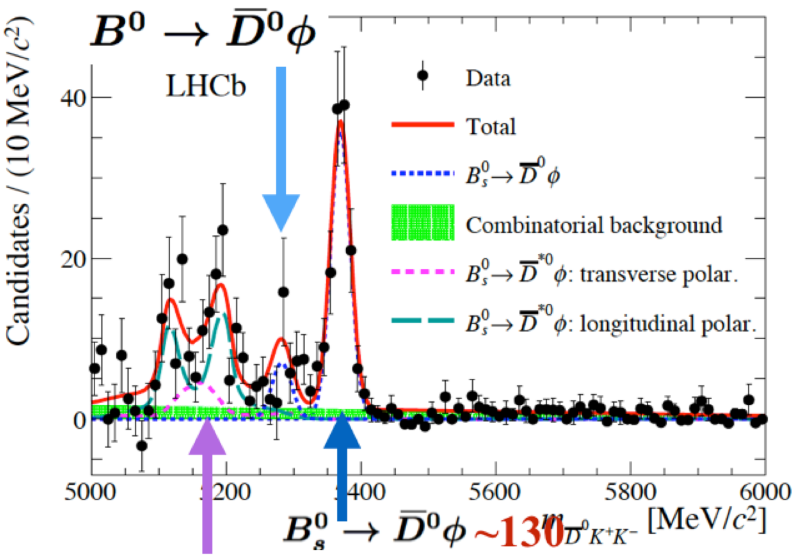


$B_s^0 \to \bar{D}^0\phi$ ~130

$B_s^0 \to \bar{D}^{*0}\phi$ (Partially reconstructed, Two polarization components) ~160

- Comparable sensitivity on $\gamma$ w.r.t. that of the golden GGSZ mode expected for $B_s \to D^{(*)}\phi$ decays and LHCb-China group are currently working on its measurements

# $\phi_s$ updates

ATLAS-CONF-2019-009
LHCb-PAPER-2019-013
LHCb-PAPER-2019-003

- B physics now attracts more interests from GPD
- We have three important updates recently: one from ATLAS ($B_s^0 \to J/\psi\ \phi$) and two from LHCb ($B_s^0 \to J/\psi\ \phi$, 4.9 fb$^{-1}$ and $B_s^0 \to J/\psi \pi^+\pi^-$, 4.9 fb$^{-1}$)
- Interesting to see that ATLAS begins to play very important role in the game

[CKMFitter, PRD 84 (2011) 033005]

- World average: $\phi_s = -0.054 \pm 0.020$ rad vs $-0.0370 \pm 0.0006$ rad from prediction

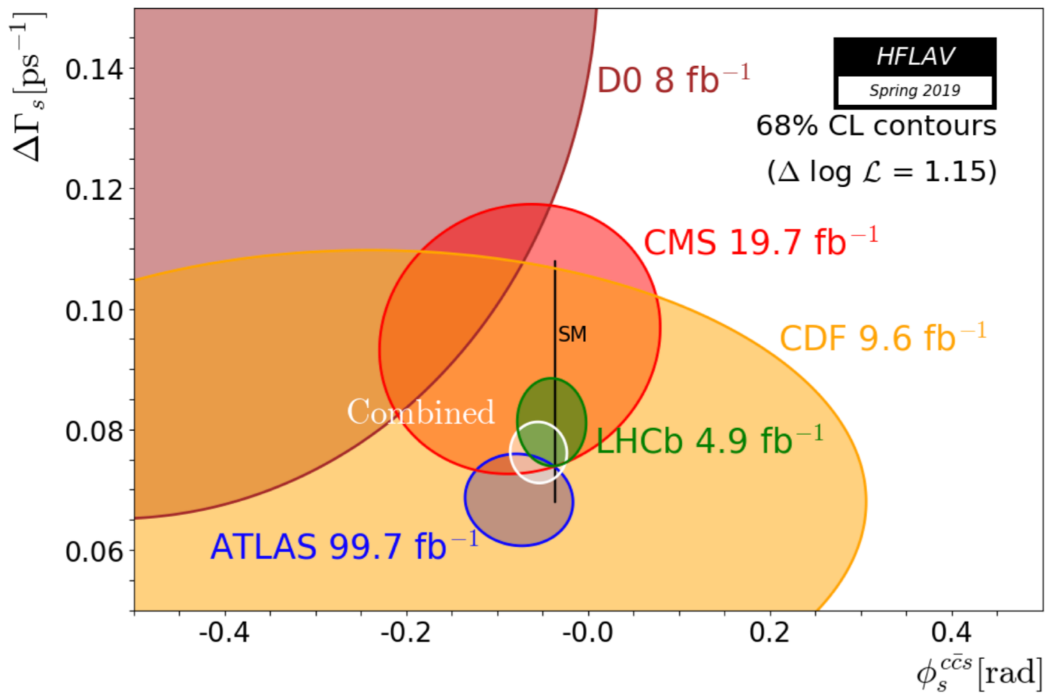

# $\phi_s^{s\bar{s}s}$ updates

LHCb-PAPER-2019-019

- Updated using 5 fb$^{-1}$ data
- SM prediction very small, ideal place to search for NP

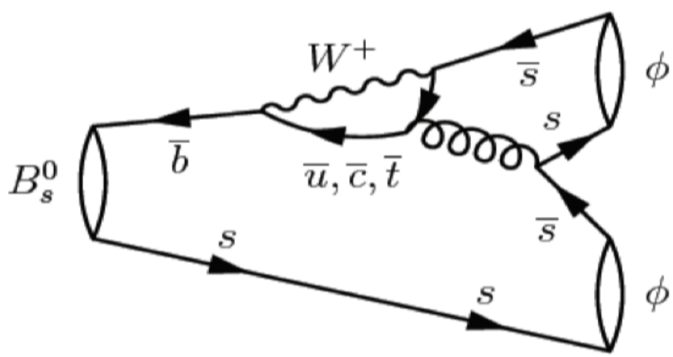


$$\phi_s^{s\bar{s}s} = -0.073 \pm 0.115 \pm 0.027 \ \text{[rad]}$$

$$|\lambda| = -0.99 \pm 0.05 \pm 0.01$$

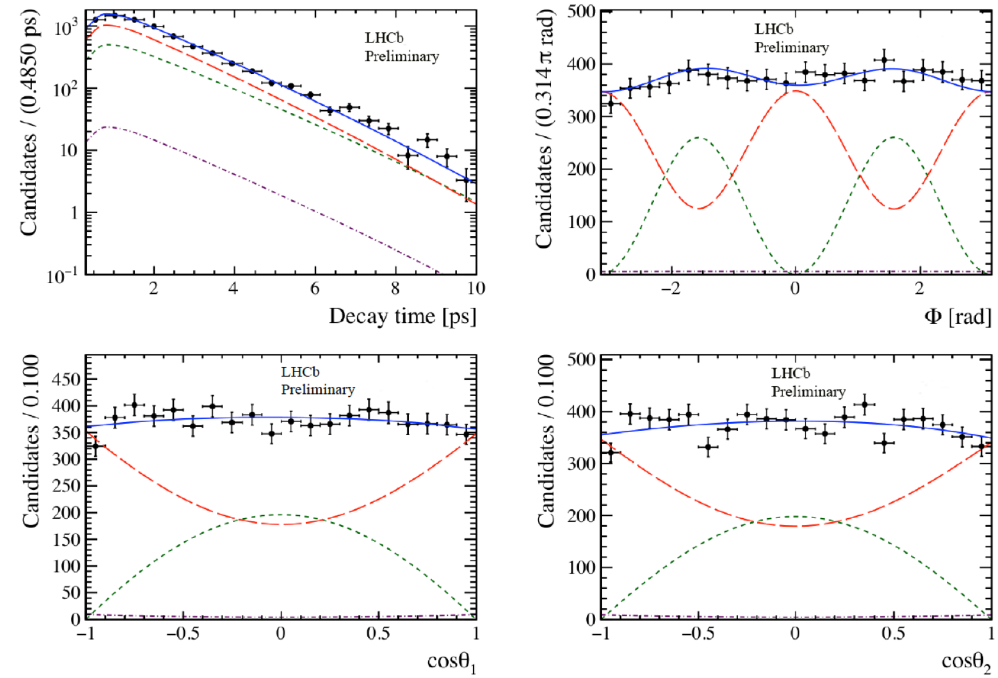


- Triple-product asymmetries also made, results consistent with no CPV
- Upper limits set for OZI suppressed mode:

$$\mathcal{B}(B^0 \to \phi\phi) < 2.7 \times 10^{-8} \ (90\,\%\ \text{CL}).$$

# CPV in charmless B decays

PRL 112 (2014) 011081
PRL 111 (2013) 101801
PRD 90 (2014) 112004

- Interesting CPV pattern seen on Dalitz plot of $B \to h'^{+}h^{+}h^{-}, h = K, \pi$
- Dalitz plot analysis needed to shed more light on understanding nature of these CPV

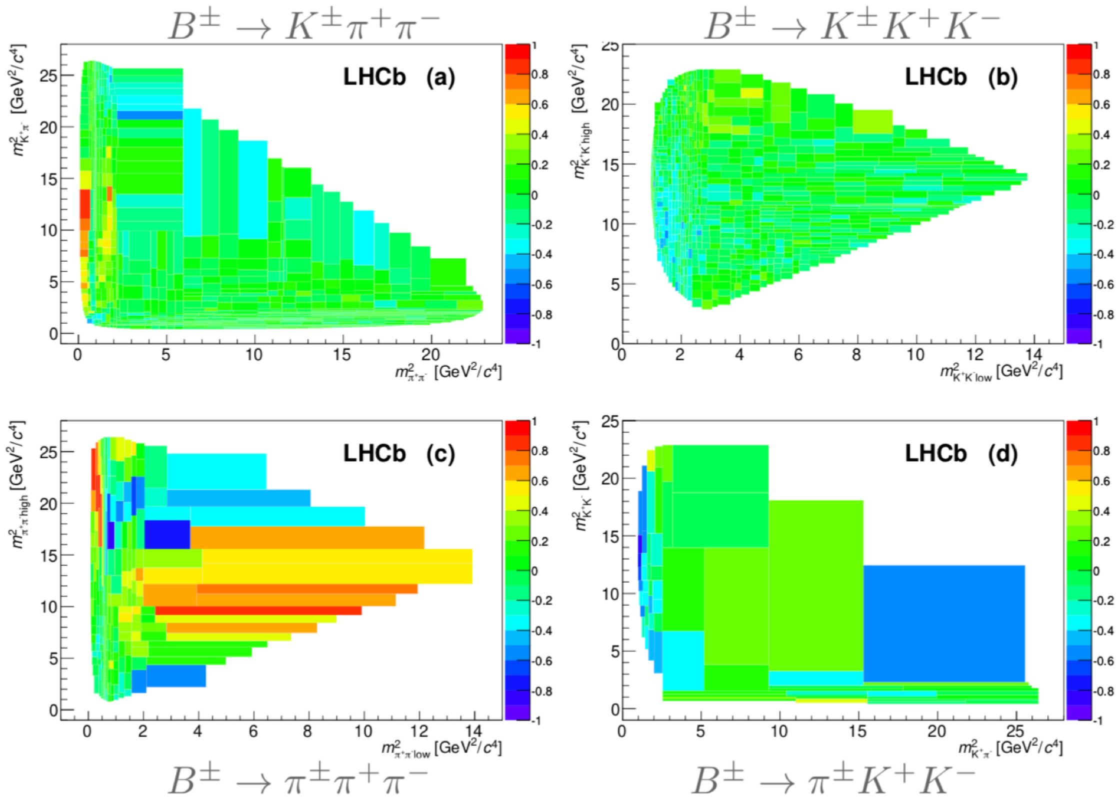


- Now, amplitude analyses of $B^{+} \to \pi^{+}\pi^{+}\pi^{-}$ and $B^{+} \to \pi^{+}K^{+}K^{-}$ , with much larger statistics than previous B-factory analyses, has been performed

# CPV over Dalitz plot

PRD 90 (2014) 112004

- Two competitive contributions needed to have CPV

$$A = a_1 e^{i(\delta_1+\phi_1)} + a_2 e^{i(\delta_2+\phi_2)} \qquad \bar{A} = a_1 e^{i(\delta_1-\phi_1)} + a_2 e^{i(\delta_2-\phi_2)}$$

$$A_{CP} = \frac{|A|^2 - |\bar{A}|^2}{|A|^2 + |\bar{A}|^2} \propto \sin(\delta_1 - \delta_2)\sin(\phi_1 - \phi_2)$$

- Distributions over PHSP offer possibilities to exam different sources of CPV

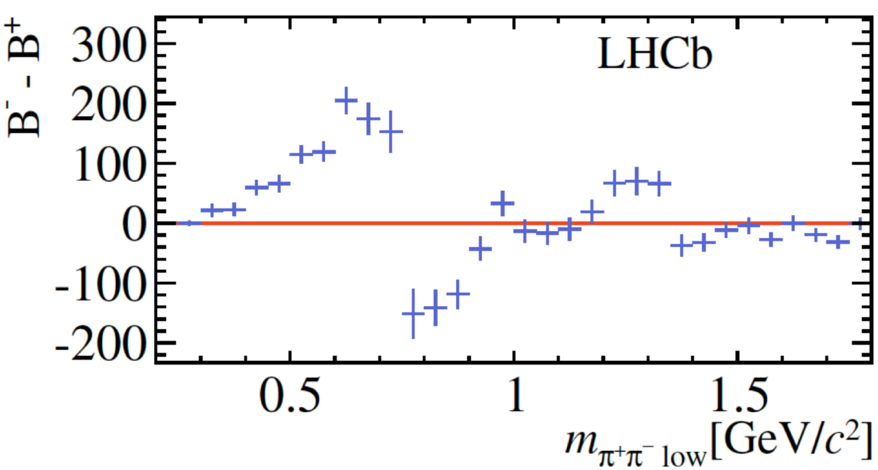


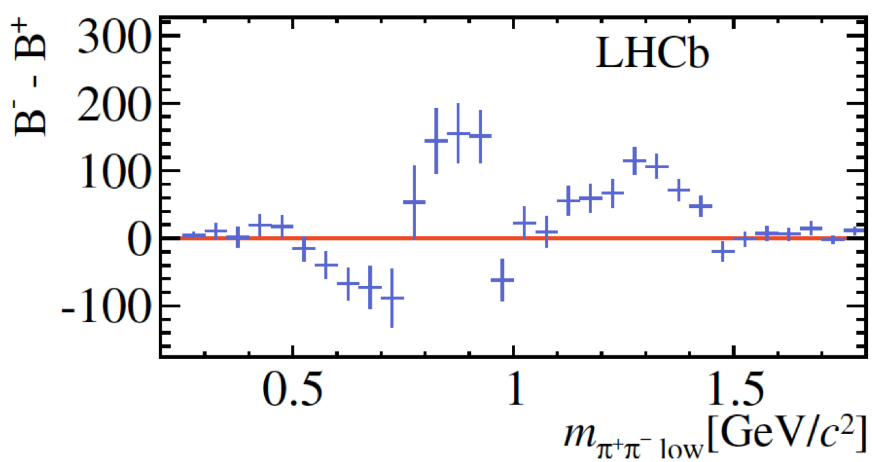

# Dalitz plot analysis with CPV

- Amplitude with CPV is modelled as

$$A(\Phi_3) = \sum_i A_i(\Phi_3) = \sum_i c_i F_i(\Phi_3)$$ Strong dynamics

$$\bar{A}(\bar{\Phi}_3) = \sum_i \bar{c}_i F_i(\Phi_3)$$ Strong + weak

- CPV then described as

$$c_i = (x_i + \Delta x_i) + i(y_i + \Delta y_i)$$
$$\bar{c}_i = (x_i - \Delta x_i) + i(y_i - \Delta y_i)$$

- Observables:

$$\mathcal{F}_i \equiv \frac{\int d\Phi_3 |A_i(\Phi_3)|^2 + \int d\Phi_3 |\bar{A}_i(\Phi_3)|^2}{\int d\Phi_3 |A(\Phi_3)|^2 + \int d\Phi_3 |\bar{A}(\Phi_3)|^2} \qquad \mathcal{A}^i_{CP} \equiv \frac{\int d\Phi_3 |\bar{A}_i(\Phi_3)|^2 - \int d\Phi_3 |A_i(\Phi_3)|^2}{\int d\Phi_3 |\bar{A}_i(\Phi_3)|^2 + \int d\Phi_3 |A_i(\Phi_3)|^2}$$

# Dalitz plot analysis with $B \to KK\pi$

PRD 90 (2014) 112004
arXiv:1905.09244

- Global CPV observed previous: $A_{cp} = -0.123 \pm 0.017 \pm 0.012 \pm 0.007$

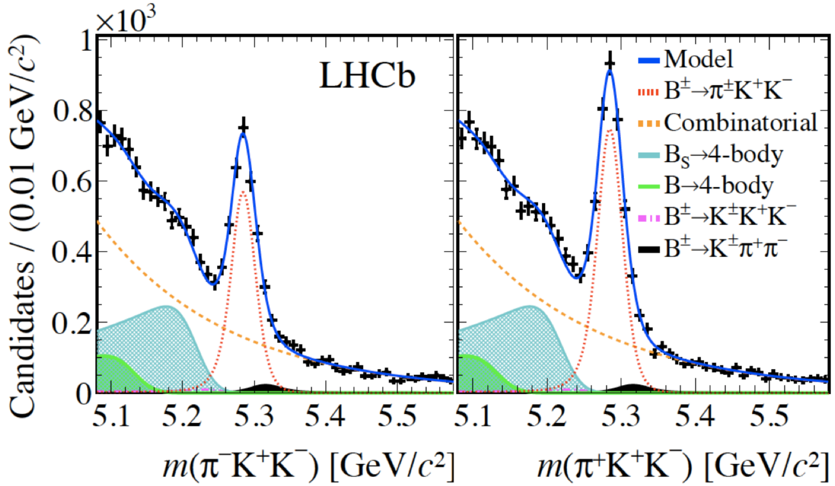


- Clear CPV found over different regions of Dalitz plot

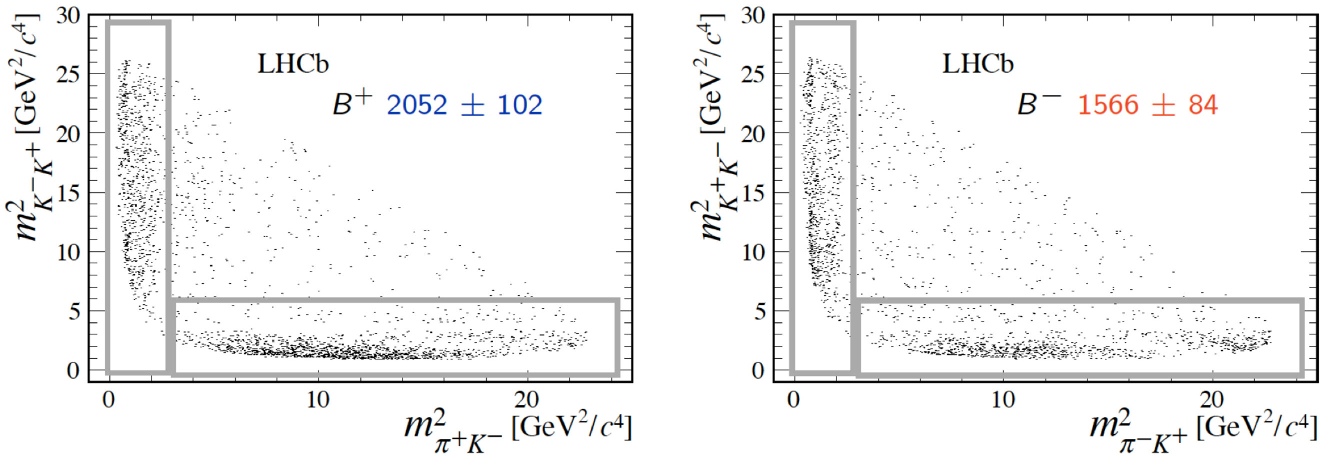

# Results: $K\pi$ resonances

arXiv:1905.09244

- Resonant contributions:

| Contribution | Fit Fraction(%) | $A_{CP}$(%) |
|---|---|---|
| $K^*(892)^0$ | $7.5 \pm 0.6 \pm 0.5$ | $+12.3 \pm 8.7 \pm 4.5$ |
| $K_0^*(1430)^0$ | $4.5 \pm 0.7 \pm 1.2$ | $+10.4 \pm 14.9 \pm 8.8$ |
| Single pole | $32.3 \pm 1.5 \pm 4.1$ | $-10.7 \pm 5.3 \pm 3.5$ |
| $\rho(1450)^0$ | $30.7 \pm 1.2 \pm 0.9$ | $-10.9 \pm 4.4 \pm 2.4$ |
| $f_2(1270)$ | $7.5 \pm 0.8 \pm 0.7$ | $+26.7 \pm 10.2 \pm 4.8$ |
| Rescattering | $16.4 \pm 0.8 \pm 1.0$ | $-66.4 \pm 3.8 \pm 1.9$ |
| $\phi(1020)$ | $0.3 \pm 0.1 \pm 0.1$ | $+9.8 \pm 43.6 \pm 26.6$ |

- $K\pi$ non-resonance modelled by

$$\mathcal{A}_{\text{source}} = \left(1 + \frac{s}{\Lambda^2}\right)^{-1}$$

$$s = m^2_{\pi^\pm K^\mp}$$
$$\Lambda = 1\,\mathrm{GeV}/c^2$$

Phys. Rev. D 92 (2015) 054010

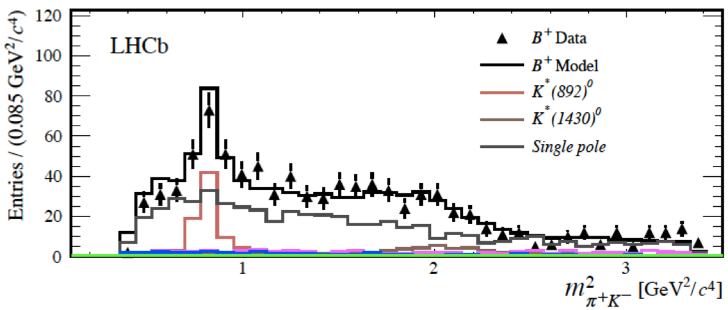


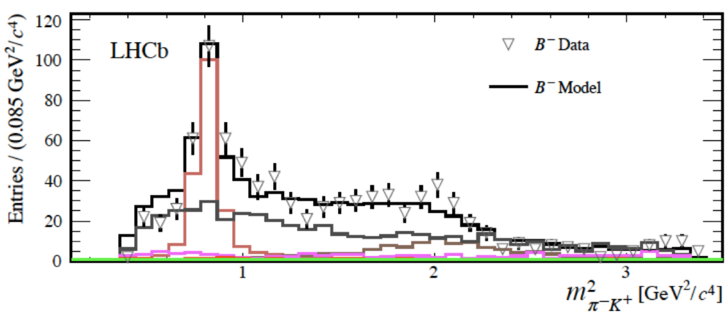

# Results: KK resonances

arXiv:1905.09244

- Resonant contributions:

| Contribution | Fit Fraction(%) | $A_{CP}$(%) |
|---|---|---|
| $K^*(892)^0$ | $7.5 \pm 0.6 \pm 0.5$ | $+12.3 \pm 8.7 \pm 4.5$ |
| $K_0^*(1430)^0$ | $4.5 \pm 0.7 \pm 1.2$ | $+10.4 \pm 14.9 \pm 8.8$ |
| Single pole | $\boxed{32.3 \pm 1.5 \pm 4.1}$ | $-10.7 \pm 5.3 \pm 3.5$ |
| $\rho(1450)^0$ | $\boxed{30.7 \pm 1.2 \pm 0.9}$ | $-10.9 \pm 4.4 \pm 2.4$ |
| $f_2(1270)$ | $7.5 \pm 0.8 \pm 0.7$ | $+26.7 \pm 10.2 \pm 4.8$ |
| Rescattering | $16.4 \pm 0.8 \pm 1.0$ | $-66.4 \pm 3.8 \pm 1.9$ |
| $\phi(1020)$ | $0.3 \pm 0.1 \pm 0.1$ | $+9.8 \pm 43.6 \pm 26.6$ |

- $KK$ non-resonance modelled by rescattering model

$$\mathcal{A}_{\text{rescattering}} = \left(1 + \frac{s}{\Lambda^2}\right)^{-1} \sqrt{1 - \nu^2}\, e^{2i\delta}$$

Phys. Rev. D 71 (2005) 074016

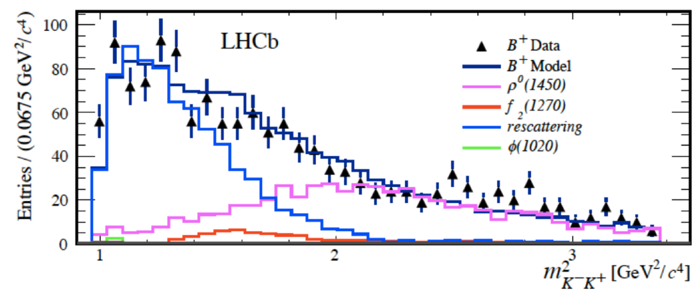


- CPV as larger as $-66.4\%$, largest CPV found in a single decay

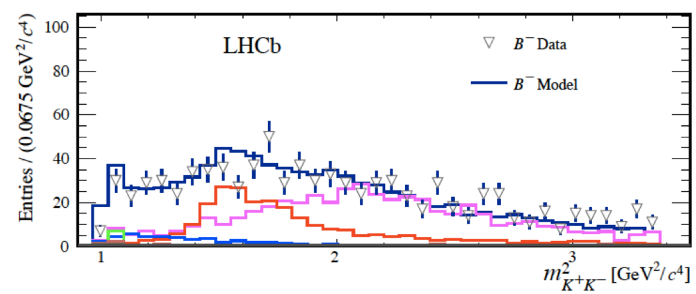

# Dalitz plot analysis with $B \to \pi\pi\pi$

LHCb-PAPER-2019-017
LHCb-PAPER-2019-018

- Dalitz plot analysis with $20594 \pm 1569$ events

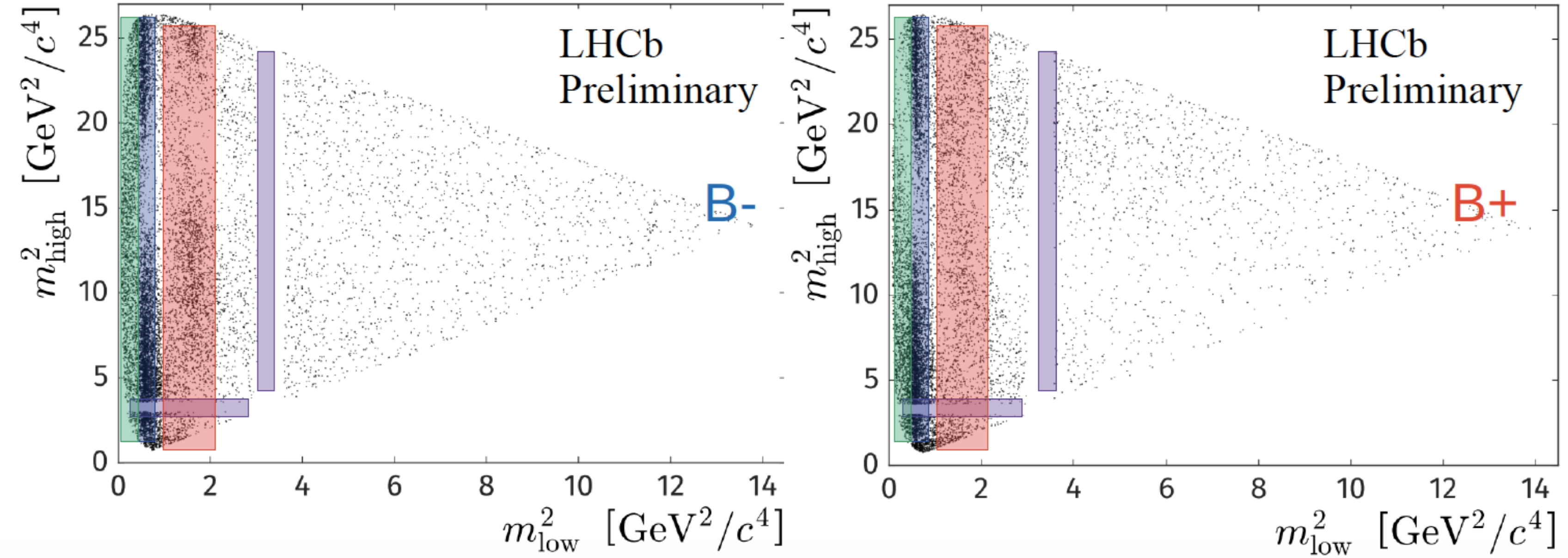


- Resonant contributions:

  $\rho$-$\omega$, $f_0(500)$, $f_0(980)$ region: S-P wave interference

  $f_2(1270)$ region: D-S, P wave interference

  High mass: KK-$\pi\pi$ rescattering

# S-wave description

LHCb-PAPER-2019-017
LHCb-PAPER-2019-018

- General agreed descriptions (RBW, GS) for $\pi\pi$ P- and D-waves;
- More complicated $\pi\pi$ S-wave, modeled in three different approaches:
  - Isobar model: different S-wave contributions are explicitly modeled:

    $f_0(500)$: RBW, complex pole parameterization

    $$\boxed{T_\sigma(m_{13}) = \frac{1}{m_\sigma^2 - m_{13}^2},}$$

    PRD 71 (2005) 054030

    **$f_0(980)$: Flatte parametrization**

    non-resonant: flat, Belle model, re-scattering model etc

    $$\boxed{T_{nr}(m_{13}, m_{23}) = c_{nr}(e^{-\alpha_{nr} m_{13}^2} e^{i\delta_1^{nr}} + e^{-\alpha_{nr} m_{23}^2} e^{i\delta_2^{nr}}),}$$

    PRL 96 (2006) 251803

    $$\boxed{T_{nr}(m_{13}) = \frac{a^{nr}}{1 + \frac{m_{13}^2}{\Lambda^2}} e^{i\delta^{nr}}}$$

    arXiv:hep-ph/1506.08332

  - K-Matrix approach: 5 poles and 5 decay channels; parameters from global fit to previous data while production vector parameters from fit to data

    EPJA 16 (2003) 229

  - Model independent approach (QMI): $\pi\pi$ S-wave binned into 13 bins; amplitudes in each bin obtained from fit to data (26 free parameters)

# S-wave results



- Good agreement between the three approaches

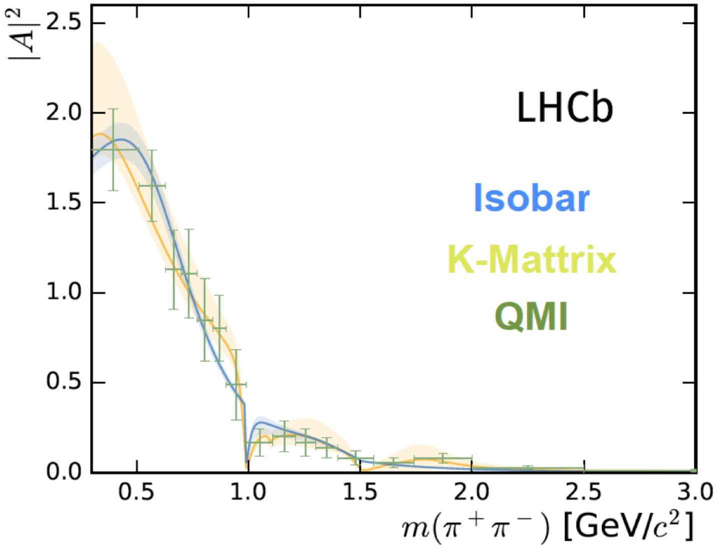


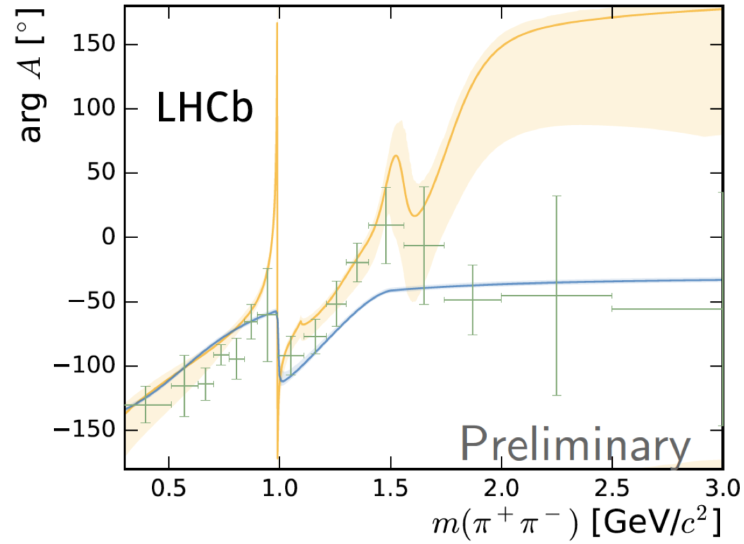


- Similar CPV pattern for the three approaches, as large as 10 $\sigma$

Isobar

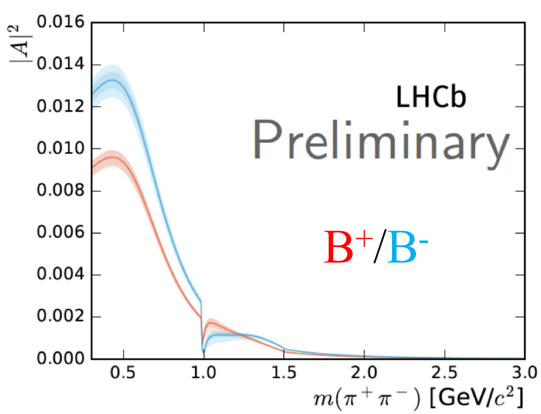


KMatrix

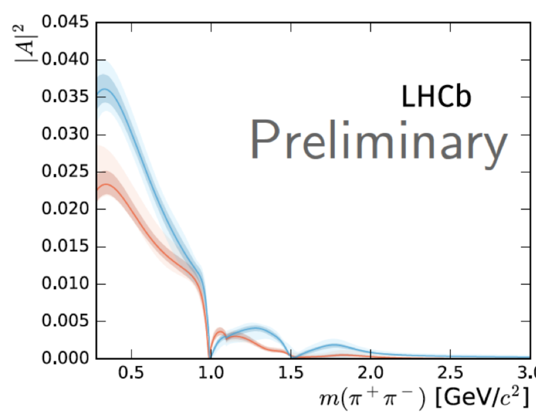


QMI

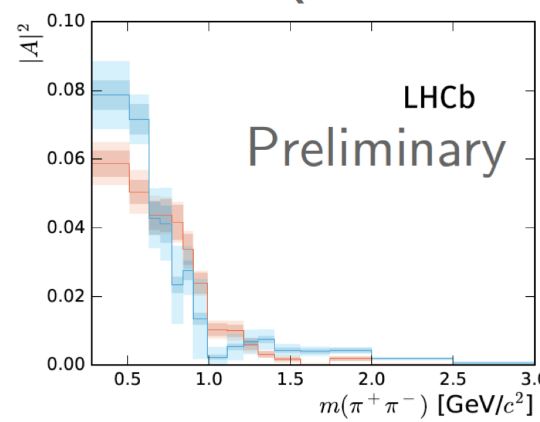

# $B \to \pi\pi\pi$ results

LHCb-PAPER-2019-017
LHCb-PAPER-2019-018

- Fit fractions:

| Component | Isobar | K-matrix | QMI |
|---|---|---|---|
| $\rho(770)^0$ | $55.5 \pm 0.6 \pm 0.7 \pm 2.5$ | $56.5 \pm 0.7 \pm 1.5 \pm 3.1$ | $54.8 \pm 1.0 \pm 1.9 \pm 1.0$ |
| $\omega(782)$ | $0.50 \pm 0.03 \pm 0.03 \pm 0.04$ | $0.47 \pm 0.04 \pm 0.01 \pm 0.03$ | $0.57 \pm 0.10 \pm 0.12 \pm 0.12$ |
| $f_2(1270)$ | $9.0 \pm 0.3 \pm 0.8 \pm 1.4$ | $9.3 \pm 0.4 \pm 0.6 \pm 2.4$ | $9.6 \pm 0.4 \pm 0.7 \pm 3.9$ |
| $\rho(1450)^0$ | $5.2 \pm 0.3 \pm 0.4 \pm 1.9$ | $10.5 \pm 0.7 \pm 0.8 \pm 4.5$ | $7.4 \pm 0.5 \pm 3.9 \pm 1.1$ |
| $\rho_3(1690)^0$ | $0.5 \pm 0.1 \pm 0.1 \pm 0.4$ | $1.5 \pm 0.1 \pm 0.1 \pm 0.4$ | $1.0 \pm 0.1 \pm 0.5 \pm 0.1$ |
| S-wave | $25.4 \pm 0.5 \pm 0.7 \pm 3.6$ | $25.7 \pm 0.6 \pm 2.6 \pm 1.4$ | $26.8 \pm 0.7 \pm 2.0 \pm 1.0$ |

- Dominant contributions from S-wave and $\rho(770)$

- CP asymmetries:

| Component | Isobar | K-matrix | QMI |
|---|---|---|---|
| $\rho(770)^0$ | $+0.7 \pm 1.1 \pm 1.2 \pm 1.5$ | $+4.2 \pm 1.5 \pm 2.6 \pm 5.8$ | $+4.4 \pm 1.7 \pm 2.3 \pm 1.6$ |
| $\omega(782)$ | $-4.8 \pm 6.5 \pm 6.6 \pm 3.5$ | $-6.2 \pm 8.4 \pm 5.6 \pm 8.1$ | $-7.9 \pm 16.5 \pm 14.2 \pm 7.0$ |
| $f_2(1270)$ | $+46.8 \pm 6.1 \pm 3.6 \pm 4.4$ | $+42.8 \pm 4.1 \pm 2.1 \pm 8.9$ | $+37.6 \pm 4.4 \pm 6.0 \pm 5.2$ |
| $\rho(1450)^0$ | $-12.9 \pm 3.3 \pm 7.0 \pm 35.7$ | $+9.0 \pm 6.0 \pm 10.8 \pm 45.7$ | $-15.5 \pm 7.3 \pm 14.3 \pm 32.2$ |
| $\rho_3(1690)^0$ | $-80.1 \pm 11.4 \pm 13.5 \pm 24.1$ | $-35.7 \pm 10.8 \pm 8.5 \pm 35.9$ | $-93.2 \pm 6.8 \pm 8.0 \pm 38.1$ |
| S-wave | $+14.4 \pm 1.8 \pm 2.1 \pm 1.9$ | $+15.8 \pm 2.6 \pm 2.1 \pm 6.9$ | $+15.0 \pm 2.7 \pm 4.2 \pm 7.0$ |

- Large CPV from S-wave and $f_2(1270)$

# New CPV pattern

LHCb-PAPER-2019-017
LHCb-PAPER-2019-018

- CPV around $\rho(770)$ pole well described by the three S-wave models

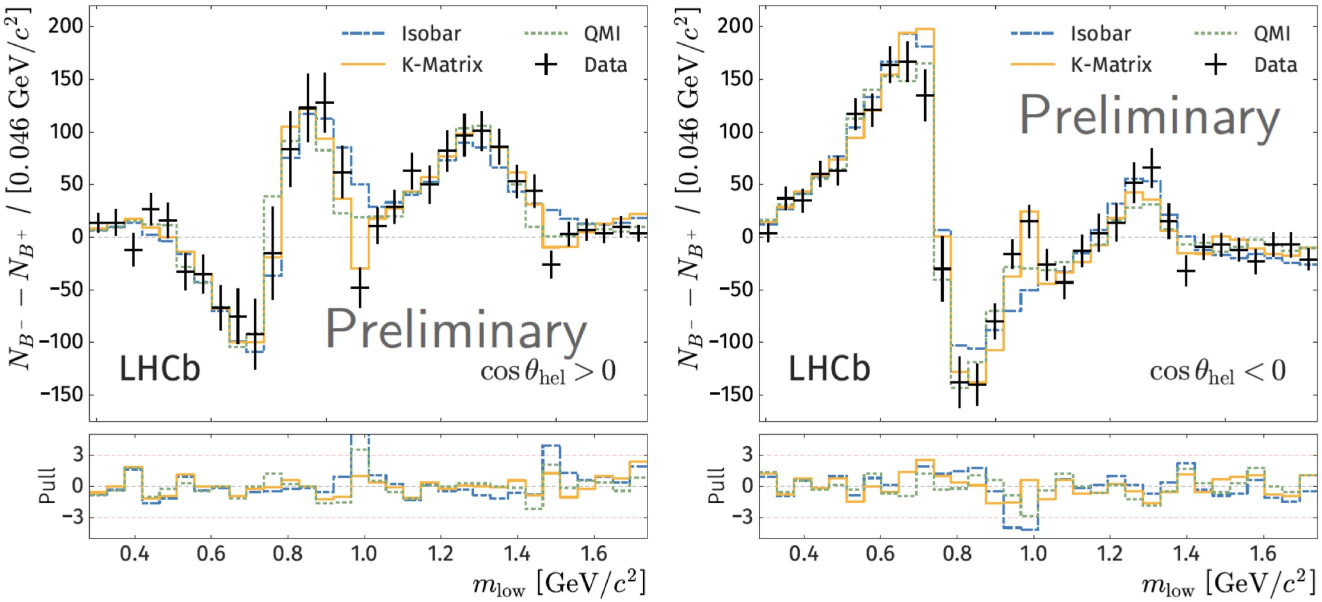


- Over 25$\sigma$ significance for CPV due to S-P interference, first observation
- Sign-flip due to phase change and helicity angle change
- First observation of large CPV in decays with tensor

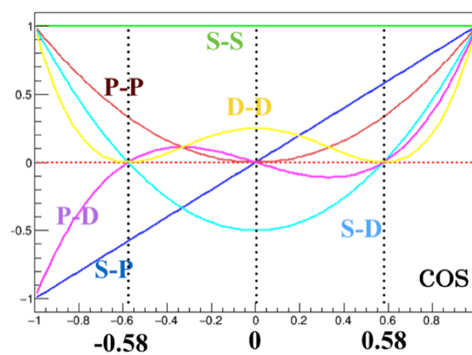


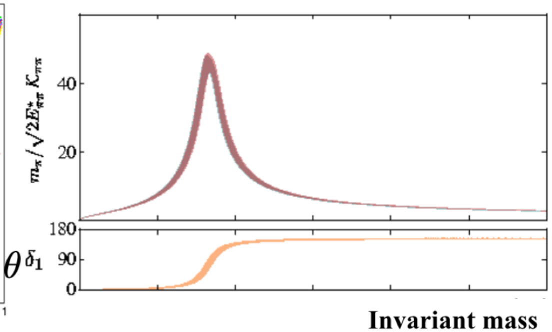

# The next CPV

Nature Physics 13 (2017) 391

- CPV has not yet been found in baryon decays
- We saw first evidence of $3.3\sigma$ 2 years ago in $\Lambda_b \to p3\pi$ using triple products

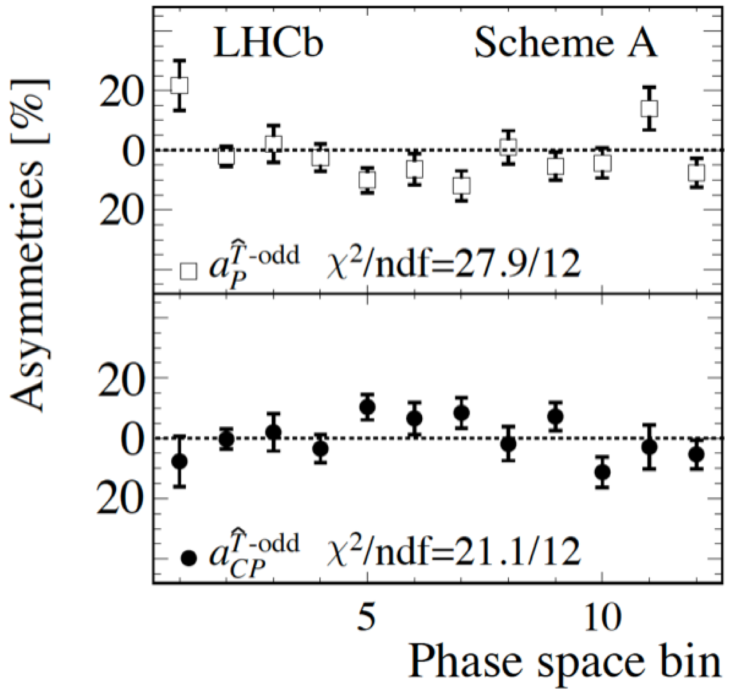


**Binning based on resonant structures, e.g. ρ(770), N*, Δ++**

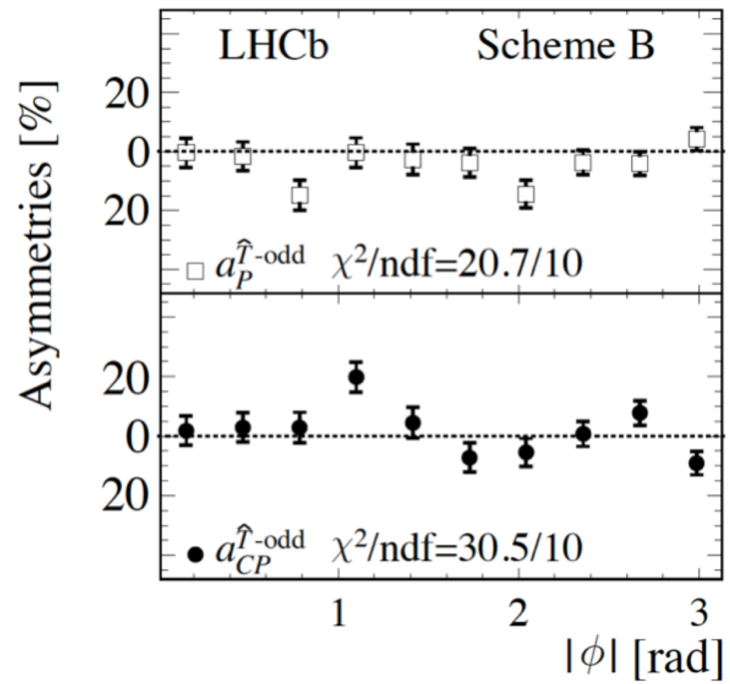


**Binning based on ϕ angle**

- Searches are performed extensively in LHCb, including $\Lambda_b \to p3\pi$, $\Lambda_b \to pK_S\pi$ (a CPV as large as 20% is predicted in arXiv:1412.1899)

# Conclusion

- Plenty of interesting CPV measurements in B decays performed by the LHCb experiments, shedding new lights on our understanding of underlying dynamics
- One of the key goals of LHCb is to search for New physics through precision measurements. New physics may appear anywhere, maybe in flavor sector in year 202x